

Supplementary material

Synthesis and Characterization of Poly(RGD) Proteinoid Polymers and NIR fluorescent Nanoparticles of Optimal D,L-Configuration for Drug Delivery Applications – In Vitro Study

*Elad Hadad^a, Safra Rudnick-Glick^a, Igor Grinberg^a, Michal Kolitz-Domb^a, Jordan H.Chill^b and
Shlomo Margel^{a*}*

^aDepartment of Chemistry, Institute of Nanotechnology & Advanced Materials, Bar Ilan
University, Ramat-Gan, Israel

^bDepartment of Chemistry, Bar Ilan University, Ramat-Gan 5290002, Israel

Supporting information including:

Figure S1. FTIR spectrum and UV-Vis absorption spectra of P(R^DGD^D, RGD, RGD^D) proteinoids.

Figure S2: 2D-NMR analysis of P(R^DGD) proteinoids.

Figure S3: NMR analysis of P(R^DGD^D, RGD, RGD^D) composition.

Figure S4: Simulations for prediction of RGD-content in P(R^DGD, R^DGD^D, RGD, RGD^D) NPs.

Table S1: NMR analysis of amino-acid incorporation into P(RGD)s.

Figure S5: Photostability of the encapsulated ICG P(R^DGD R^DGD^D, RGD, RGD^D) NPs and Free ICG

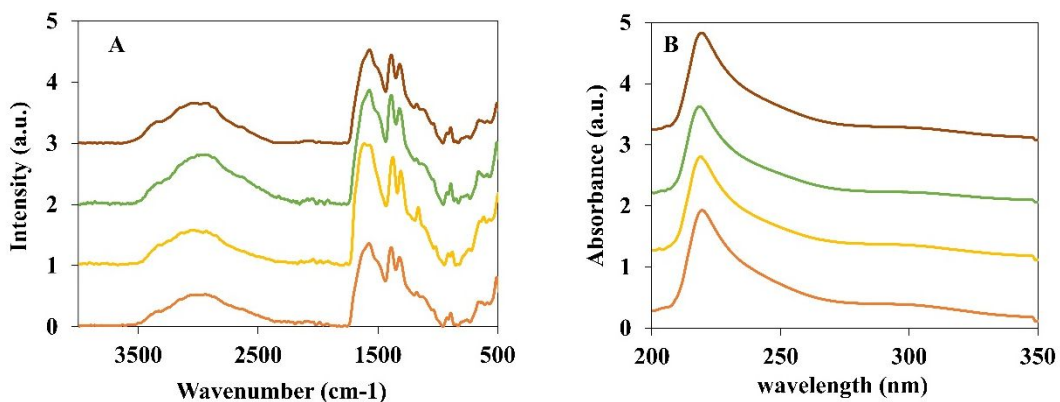


Figure S1. FTIR spectrum (A) and UV-Vis absorption spectra (B) of, P(R^DGD R^DGD^D), RGD, RGD^D) proteinoids (orange, yellow, green, brown) respectively.

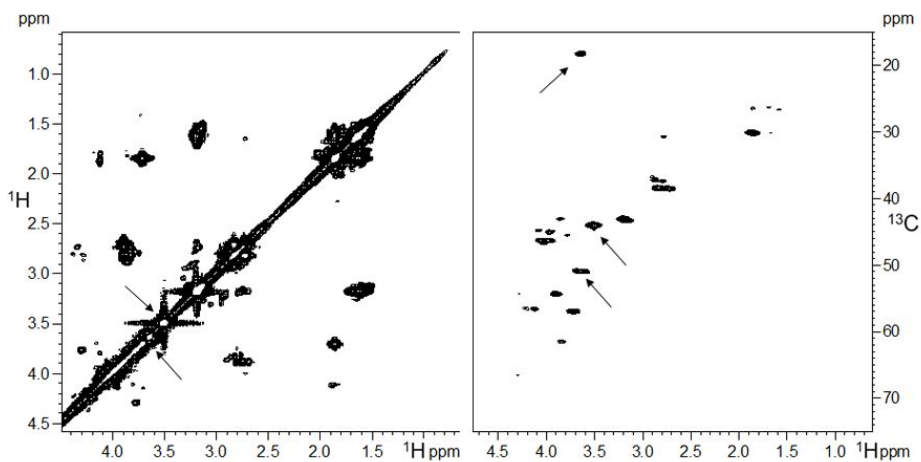


Figure S2. 2D-NMR analysis of P(R^DGD) proteinoids. Left, 2D homonuclear COSY spectrum of P(R^DGD), and right, 2D ¹H-¹³C-HMQC spectrum of P(R^DGD), both acquired for a 10 mg/ml sample in ²H₂O at 300 K and 16.4 T. Analysis of these spectra and comparison to expected correlation cross-peaks of the three amino acids allowed specific peaks (marked with arrows) to be identified as non-proteinoid signals and to be excluded from the integration analysis.

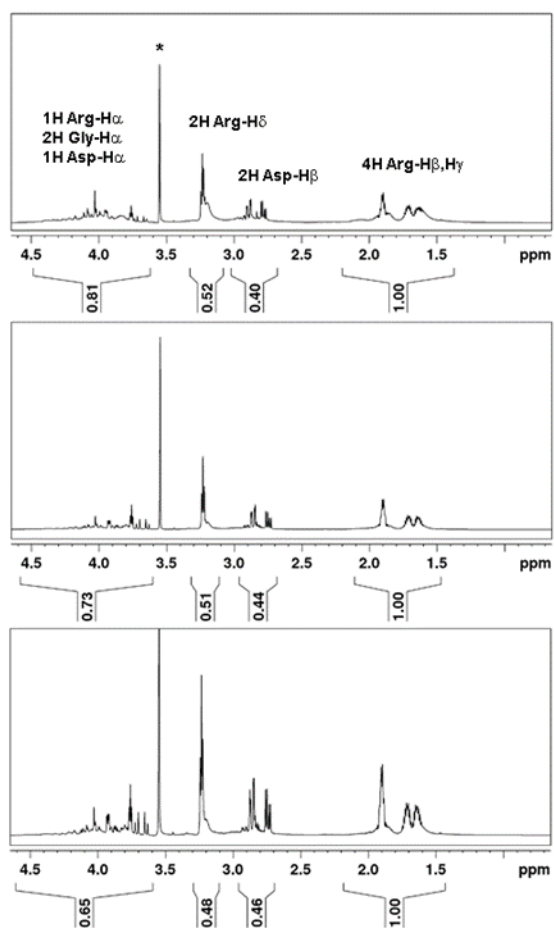


Figure S3. NMR analysis of $\text{P}(\text{R}^{\text{D}}\text{GD})$ proteinoid amino acid composition. Similarly to Figure 1, $^1\text{D } ^1\text{H-NMR}$ spectrum of 10 mg/ml proteinoid in $^2\text{H}_2\text{O}$ were acquired at 300 K and 16.4 T. Signals emanating from arginine, glycine and aspartate protons as well as integrated signal areas are shown. Asterisks denote non-proteinoid peaks excluded from the integration analysis. **Top**, $\text{P}(\text{R}^{\text{D}}\text{GD}^{\text{D}})$, **Middle**, $\text{P}(\text{R}\text{GD}^{\text{D}})$, **Bottom**, $\text{P}(\text{R}\text{GD})$.

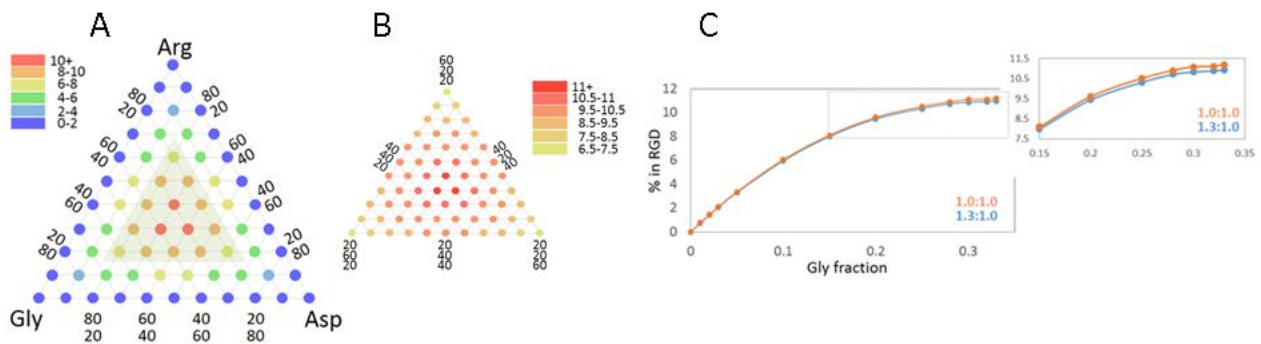


Figure S4. Simulations for prediction of RGD content using amino acid composition. Based on the NMR-derived amino acid composition, random polypeptides were simulated and RGD occurrences counted. These are presented in a ternary component graph. **(A)** Percentage of residues involved in RGD triads as a function of the amino acid composition. **(B)** Detailed presentation of central region (shaded grey triangle) of the graph in (A). The color scale shows the %RGD for each point in the ternary graph. **(C)** Expected levels of residue involvement in RGD triads for conditions prevalent in this study as a function of the Gly mol:mol fraction when Arg:Asp is 1:1 (blue) and when Arg:Asp is 1.3:1 (orange), representing the range of ratios seen in our P(RGD)s.

Table S1a: NMR analysis of amino-acid composition in P(R^DGD^D)

ppm-1	ppm-2	¹ H nuclei	Relative intensity	Normalized intensity ^a
1.25	2.21	4H Arg ^D (H ^β ,H ^γ)	1.00	0.25
2.60	3.02	2H Asp ^D (H ^β)	0.40	0.20
3.04	3.32	2H Arg ^D (H ^δ)	0.52	0.26
3.56	4.41	1H Arg ^D (H ^α), 2H Gly(H ^α), 1H Asp ^D (H ^α)	0.81 ^b	Arg ^D – 0.25 ^c Gly – 0.18 Asp ^D – 0.20 ^c

Table S1b: NMR analysis of amino-acid composition in P(RGD^D)

PPM-1	PPM-2	¹ H nuclei	Relative intensity	Normalized intensity ^a
1.25	2.21	4H Arg(H ^β ,H ^γ)	1.00	0.25
2.60	3.02	2H Asp ^D (H ^β)	0.44	0.22
3.04	3.32	2H Arg(H ^δ)	0.51	0.255
3.56	4.41	1H Arg (H ^α), 2H Gly(H ^α), 1H Asp ^D (H ^α)	0.73 ^b	Arg – 0.25 ^c Gly – 0.13 Asp ^D – 0.22 ^c

Table S1c: NMR analysis of amino-acid composition in P(RGD)

PPM-1	PPM-2	¹ H nuclei	Relative intensity	Normalized intensity ^a
1.25	2.21	4H Arg(H ^β ,H ^γ)	1.00	0.25
2.60	3.02	2H Asp(H ^β)	0.46	0.23
3.04	3.32	2H Arg(H ^δ)	0.48	0.24
3.56	4.41	1H Arg(H ^α), 2H Gly(H ^α), 1H Asp(H ^α)	0.65 ^b	Arg – 0.25 ^c Gly – 0.085 Asp – 0.23 ^c

^a Signal intensity per proton nucleus.

^b Excluding the signals from solvent impurities at 3.57/3.65 ppm.

^c Relative contributions of Arg/Gly/Asp were based on the appropriate stoichiometric ratios.

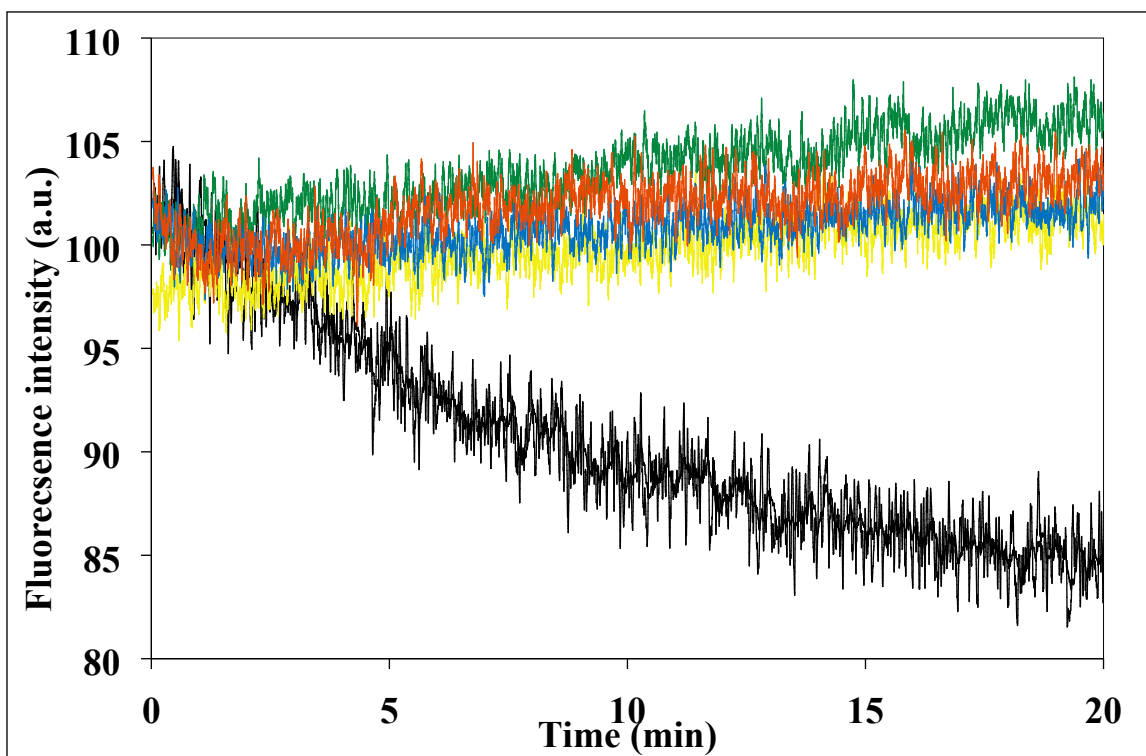


Figure S5. Photostability of the encapsulated ICG P(R^DGD R^DGD^D, RGD, RGD^D) NPs and Free ICG. Illumination was performed continuously at 780 nm for a period of 30 minutes, for all the four different configurations of the ICG-encapsulated P(R^DGD, R^DGD^D, RGD, RGD^D) NPs and were compared to the photostability of the free ICG. **(Red)** ICG-encapsulated P(R^DGD^D) NPs, **(blue)** ICG-encapsulated P(RGD) NPs, **(green)** ICG-encapsulated P(R^DGD) NPs, **(yellow)** ICG-encapsulated P(RG^DD) NPs, **(black)** free ICG.